# Electromagnetic shunt damping with negative impedances: Optimization and analysis

Shaoyi Zhou, Claire Jean-Mistral, Simon Chesné

Version of Record: https://www.sciencedirect.com/science/article/pii/S0022460X19300227
Manuscript_bed8cda3cd7d2ca955a0c430706e4b59

# Electromagnetic shunt damping with negative impedances: optimization and analysis

Shaoyi Zhou, Claire Jean-Mistral, Simon Chesne*

*Université de Lyon, CNRS INSA-Lyon, LaMCoS UMR5259, 69621 Villeurbanne, France*

**Abstract**

Dynamic vibration absorbers (DVA) are classic and effective devices to reduce the amplitude of vibration sustained by structures. A promising alternative to the DVAs is the electromagnetic shunt damper (EMSD), in which the electrical shunt circuit serves as the absorbing oscillator. The objective of this paper is to carry out optimum designs of an EMSD connected to a resistive-inductive-capacitive (RLC) shunt circuit, by adopting three different calibration strategies: the fixed points theory, $H_2$ optimization criterion and maximum damping criterion. The aforementioned optimization strategies are appropriate to different excitation scenarios: harmonic, random and transient vibration, respectively. Analytical expressions of optimal parameters are formulated in terms of the ratio of external inductance in the shunt and inherent inductance of electromagnetic transducer. Lower bounds of inductance ratio in the region of stability are also specified for each strategy, based on which the ultimate attainable performance of EMSDs can be predicted. Numerical investigation underlines that including a negative inductance in the shunt always contributes to reduce the frequency response magnitude, broaden the absorbing area around targeted vibration mode, increase the damping performance, and thereby accelerate the decay rate of transient vibration.

*Keywords:* Electromagnetic shunt damping, negative impedances, optimum design, fixed points theory, $H_2$ optimization criterion, maximum damping criterion

## 1. Introduction

When subjected to environmental disturbances, mechanical systems may undergo undesirable vibrations which could result in potential damages to the structure. Therefore, vibration damping is an important issue in lots of domains, such as transport, energy and civil structure. The most popular and reliable anti-vibration device is probably the classic DVA [1], which can be modelled as a mass-spring-damper system and is attached to the primary structure to reduce its vibration. Despite its simplicity and effectiveness, DVA presents two obvious limitations: increase of total mass of system due to the mechanical oscillator and need of large volume due to the moving part.

The tuning of DVAs has been widely investigated since the first half of last century. Den Hartog studied its optimum design under harmonic vibration and introduced the well-known fixed points theory in his book *Mechanical Vibrations* [2]. This pioneering theory considers that under harmonic vibration, the frequency response of undamped primary structure will always pass through two invariant points regardless of damping introduced by the auxiliary oscillator, and the optimal system parameters should be selected in such a way

*Corresponding author
*Email address:* simon.chesne@insa-lyon.fr (Simon Chesne)

that the two invariant points are global maximum and have equal magnitudes. In fact, this empirical technique only conducts to an approximative solution to the $H_\infty$ optimization problem, which aims at minimizing the maximum amplitude of frequency response. The exact method had not been proposed until Nishihara et al. [3] adopted an algebraic approach to successfully solve this problem in 2002. When subjected to broadband random vibration, one can note that the area under the frequency response curve of primary system should be minimized instead of displacement magnitudes at certain discrete frequencies [4]. Hence, the objective function for the $H_2$ optimization problem is the squared norm of frequency response of the primary structure, and analytical solutions were proposed by Asami et al. for undamped [5] and damped primary structure [6] under random vibration. Another common excitation scenario is that the main system undergoes short-term disturbances. In this case, the maximum damping criterion should be adopted, which aims at decreasing the transient response as fast as possible. This criterion is based on pole placement technique, and is widely used in the field of shunt damping with smart materials [7, 8], or vibration control of civil structures [9]. Given that the decay rate of transient response is governed by the real part of eigenvalues of coupled system, maximizing the absolute values of real parts of roots will reduce the transient vibration response in a minimum time.

In the past few decades, numerous alternatives to the DVAs have been proposed, such as electromechanical shunt dampers [10–12], which are connected with an electrical shunt circuit, and are usually localized between the primary structure and its base. In this way, the absorbing oscillator is electrical and can be fine-tuned to attenuate vibrations of the structure.

Hagood and von Flotow [7] proposed to attenuate the vibrations of a cantilever beam by using a piezoelectric patch shunted with a resistive-inductive (RL) series impedance. In their work, both the $H_\infty$ optimization criterion (fixed points theory) and the pole placement technique were adopted to obtain optimal parameters. By using these two methods, Caruso [8] performed optimization analyses and conducted a performance comparison for three shunt circuits, RL in series, RL in parallel and series RL in parallel with a capacitor (RLC parallel). It was demonstrated that compared to the RL series circuit, the positive parallel capacitance will significantly deteriorate the shunt damping performance; further details about the influence of positive capacitances in the shunt and methods to avoid the problem can be found in [13–15]. Therefore, one can imagine that a negative capacitance could be included in the shunt impedance to improve the damping performance and enhance its robustness [16–20]. Indeed, the negative capacitance contributes to artificially enhance the electromechanical coupling so that the achievable attenuation will be increased [16, 19, 21].

Analogous to piezoelectric shunt damping, Behrens et al. [22, 23] proposed the concept of electromagnetic shunt damping. Compared to its piezoelectric counterpart, the electromagnetic transducers present some benefits: smaller shunt voltages, larger control forces, larger strokes and more robustness [22–24]. By adopting the fixed points theory, Inoue et al. [25] analytically derived optimal parameters of EMSDs connected with an either resistive (R) or resistive-capacitive (RC) shunt circuit in the harmonic vibration scenario. Tang et al. [26] determined exact solutions to both $H_\infty$ and $H_2$ optimization problems for an EMSD connected with a RC series shunt circuit. Similar to the case of piezoelectric shunt damping, negative impedances can be also adopted in the electromagnetic shunt damping. As pointed out in Ref. [22], the electromagnetic transducer can be modelled as an inductor, a resistor and a velocity-controlled voltage source in series. Hence, a negative resistance and/or a negative inductance can be employed in the shunt circuits. In this way, the total electrical impedance of EMSD will be reduced so that the current in the circuit will increase, which thereby results in the improvement of damping performance. Under the guidance of this idea, fruitful researches were conducted on

electromagnetic shunt damping with negative impedances [27–32]. Niu et al. [27] investigated vibration damping of a cantilever beam under harmonic excitation by using a C shunt or a RC series shunt with a negative resistance, which demonstrated that the latter one provides better attenuation performance than the purely capacitive shunt. Yan et al. [28] designed a novel isolator based on EMSD with a negative resistance, which can suppress vibration effectively under both sinusoidal and half-cycle sine pulse excitation. In Ref. [29, 30], a shunt impedance composed of a negative inductance and a negative resistance in series was used to suppress multimodal vibration of a cantilever plate and the transverse vibration of a cantilever beam. It has been proven in [29, 30] that compared to a traditional DVA, an EMSD with negative impedances can attenuate vibration on multiple modes, and it presents the advantage of structural simplicity compared to active shunt absorbers, where a feedback system is indispensable and complicated control algorithms are required for real-time adjustment.

The authors remark that no research has yet been conducted on optimization of EMSDs with a negative inductance in series with a RC shunt circuit. In order to fill this gap in the current literature, an EMSD shunted with a RLC series circuit will be investigated and optimum designs will be conducted in three aforementioned excitation scenarios corresponding to three different criteria: fixed points theory (FPT), $H_2$ optimization criterion and maximum damping criterion (MDC). By comparing with the existing literature, we seek to validate the proposed study and depict the influence of the additional negative inductance on damping performance of resonant EMSDs.

This paper is organized as follows. Section 2 presents the mathematical modelling of an undamped mechanical system controlled by a resonant EMSD and recasts it into a dimensionless form. Section 3 is contributed to the optimum design according to each calibration. In the next section, a detailed numerical investigation will be carried out to compare the performance of EMSD with different optimal parameters in various excitation scenarios.

## 2. Mathematical modelling

As sketched in Fig. 1, the undamped primary system is represented by a generic mass-spring model of single degree of freedom (SDOF). The electromagnetic transducer consists of a permanent magnet, an electric conductor (in the form of coil) which is shunted by a closed circuit. When subjected to external excitation, the relative velocity between the magnet and coil results in the change of the magnetic flux enclosed by the coil, which further induces a voltage across the terminals of coil. According to the Faraday-Lenz law, the induced voltage $V_i$ is related to the relative velocity by

$$V_i = Bl\dot{x} = k_v\dot{x} \tag{1}$$

where $B$ represents the magnetic flux, $l$ denotes the effective length of winding, the dot stands for differentiation with respect to time $t$, $x$ indicates the displacement of coil relative to the magnetic field, namely the displacement of main structure relative to its base, $k_v$ is defined as voltage constant of electromagnetic transducer and the subscript $i$ refers to induced/inherent property. The electric current generated in the coil will produce a Lorentz force $F_i$, which is opposite in direction to the relative velocity and proportional in magnitude to the current, i.e.

$$F_i = k_f\dot{q} \tag{2}$$

where $k_f$ stands for the force constant of electromagnetic transducer and $q$ is the electric charge flowing into the external impedance. It is worth noting that this reaction force $F_i$ usually opposes the relative motion between

the permanent magnet and the coil, hence it acts as a damping force. Besides, the relationship between $k_v$ and $k_f$ is usually simplified as $k_v = k_f = k_e$ [33].

The electromagnetic transducer can be modelled as a resistor $R_i$, an inductor $L_i$ and a velocity-controlled voltage source $V_i$ in series, as shown in Fig. 2. In this study, the inherent inductance $L_i$ is supposed to be irrelevant to the changes of magnetic boundary conditions of the magnetic material and is considered as constant.

Therefore, the dynamics of an undamped primary structure of SDOF under force excitation $f(t)$, coupled to an EMSD shunted with a RLC series circuit, can be described by the following equations of motion:

$$M_s\ddot{x} + K_s x + F_i = f(t) \tag{3a}$$

$$L\ddot{q} + R\dot{q} + \frac{1}{C}q - V_i = 0 \tag{3b}$$

where $M_s$ is the equivalent mass, $K_s$ is the mechanical stiffness and $C$ denotes the capacitance. Moreover, $R = R_i + R_e$ and $L = L_i + L_e$ designate the total resistance and inductance in the circuit, where the subscript $e$ refers to external shunt impedances.

In order to facilitate the following optimum designs, a series of system constants and dimensionless parameters are introduced as follows:

$$\begin{aligned} &\kappa = \frac{R_i}{L_i\omega_s}, \quad \theta = \frac{k_e}{\sqrt{K_s L_i}}, \quad \omega_s = \sqrt{\frac{K_s}{M_s}}, \quad \omega_e = \frac{1}{\sqrt{LC}}, \\ &\alpha = \frac{\omega}{\omega_s}, \qquad \beta = \frac{R_e}{R_i}, \qquad \gamma = \frac{L_e}{L_i}, \qquad \phi = \frac{\omega_e}{\omega_s}. \end{aligned} \tag{4}$$

where $\kappa$ is a constant depending only on inherent system parameters and $\theta$ stands for the electromagnetic coupling coefficient. $\omega_s$ and $\omega_e$ denote the resonant frequencies in the mechanical and electrical domains respectively. Besides, $\alpha$ is the forcing frequency normalized by the natural frequency, $\beta$ (or $\gamma$) denotes the ratio of external and internal resistance (or inductance), $\phi$ represents the frequency tuning ratio. One can note that this electromechanical system can be now described by merely two parameters, $\kappa$ and $\theta$, instead of five physical properties ($M_s$, $K_s$, $k_e$, $R_i$ and $L_i$). Finally, by substituting Eqs. (1) and (2) into Eq. (3) and rescaling the time $t$ by $t = \tau/\omega_s$ and the electrical state variable $q$ by $q = y\sqrt{M_s/L_i}$, the equations of motion (3) can be conveniently rewritten in a dimensionless form:

$$x'' + x + \theta y' = f(\tau)/K_s \tag{5a}$$

$$(1+\gamma)y'' + \kappa(1+\beta)y' + (1+\gamma)\phi^2 y = \theta x' \tag{5b}$$

where the superscript $'$ indicates differentiation with respect to dimensionless time $\tau$. Therefore, the following optimization procedure will be performed with regard to the normalized forcing frequency $\alpha$, resistance ratio $\beta$, inductance ratio $\gamma$ and frequency tuning ratio $\phi$. Besides, the electrical damping ratio $\xi_e$ is introduced here:

$$\xi_e = \frac{R}{2L\omega_s} = \frac{\kappa(1+\beta)}{2(1+\gamma)} \tag{6}$$

Denoting the complex magnitudes of displacement $x$ and force $f$ by $X$ and $F$, respectively, the frequency response function (FRF) is then defined as:

$$\mathrm{H}(\bar{s}) = \frac{X}{F/K_s} = \frac{(1+\gamma)\phi^2 + \kappa(1+\beta)\bar{s} + (1+\gamma)\bar{s}^2}{(1+\gamma)\phi^2 + \kappa(1+\beta)\bar{s} + [(1+\gamma)(1+\phi^2) + \theta^2]\bar{s}^2 + \kappa(1+\beta)\bar{s}^3 + (1+\gamma)\bar{s}^4} \tag{7}$$

where $\bar{s} = s/\omega_s = j\omega/\omega_s = j\alpha$ with $j = \sqrt{-1}$. And the squared magnitude of the FRF is formulated as:

$$\mathrm{H}^2(\alpha) = \left|\frac{X}{F/K_s}\right|^2 = \frac{(1+\gamma)^2(\phi^2-\alpha^2)^2 + \alpha^2\kappa^2(1+\beta)^2}{[(1+\gamma)(1-\alpha^2)(\phi^2-\alpha^2) - \theta^2\alpha^2]^2 + \alpha^2\kappa^2(1+\beta)^2(1-\alpha^2)^2} \tag{8}$$

The dimensionless equations of motion (5) is used to study the dynamics of coupled system in temporal domain, the FRF function (7) is employed as objective function in optimum design under random vibration and its squared magnitude (8) is adopted to minimize the $H_\infty$ norm of frequency response. These general formulations can be easily adapted to some simpler electrical networks, e.g. R shunt, RL shunt and RC shunt by imposing $\gamma = \phi = 0$, $\phi = 0$ and $\gamma = 0$, respectively.

## 3. Closed-form solutions to optimization of EMSDs

In this section, the optimization of resonant EMSDs will be carried out based on Eqs. (5) and (7) according to different optimization criteria. The ultimate performance of shunt damper will be also determined in each optimization scenario. Given that negative impedances will be probably employed in the shunt circuits, it is then essential to perform a stability analysis of the electromechanical system in order to clarify the general constraint on negative impedances.

### *3.1. Stability conditions*

By taking $\mathbf{Z} = (x, y, x', y')^\top$ as state vector, the dimensionless equations of motion (5) can be recast into a matrix form, i.e.:

$$\mathbf{Z}' = \mathbf{A}\mathbf{Z} + \mathbf{b} \tag{9}$$

where $\mathbf{b}$ only contains external forcing terms and $\mathbf{A}$ represents the system matrix relevant to the dimensionless system, which is expressed as:

$$\mathbf{A} = \begin{bmatrix} 0 & 0 & 1 & 0 \\ 0 & 0 & 0 & 1 \\ -1 & 0 & 0 & -\theta \\ 0 & -\phi^2 & \dfrac{\theta}{1+\gamma} & -\dfrac{\kappa(1+\beta)}{1+\gamma} \end{bmatrix} \tag{10}$$

Denoting $\lambda$ the eigenvalues of the system, the corresponding characteristic polynomial is then calculated by the determinant as follows:

$$\det(\mathbf{A} - \lambda\mathbf{I}) = \lambda^4 + \delta_1\lambda^3 + \delta_2\lambda^2 + \delta_3\lambda + \delta_4 \tag{11}$$

where coefficients are all real and are expressed as:

$$\delta_1 = \frac{\kappa(1+\beta)}{1+\gamma}, \quad \delta_2 = 1 + \phi^2 + \frac{\theta^2}{1+\gamma}, \quad \delta_3 = \frac{\kappa(1+\beta)}{1+\gamma}, \quad \delta_4 = \phi^2. \tag{12}$$

According the Routh-Hurwitz stability criterion, the electromechanical system is asymptotically stable if and only if all of the roots of its characteristic polynomial (11) lie in the left half of the complex plane. Precisely, the necessary and sufficient conditions are formulated as:

$$\left.\begin{array}{c} \delta_1 > 0 \\ \delta_3 > 0 \\ \delta_4 > 0 \\ \delta_1\delta_2\delta_3 > \delta_3^2 + \delta_1^2\delta_4 \end{array}\right\} \quad \Longrightarrow \quad \left\{\begin{array}{l} \beta > \beta_{\mathrm{cri}} = -1 \\ \gamma > \gamma_{\mathrm{cri}} = -1 \end{array}\right. \tag{13}$$

which implies that the absolute value of negative resistance (or inductance) should be always less than that of inherent impedances of electromagnetic transducer for the RLC series shunt circuit. It is worth noting that more strict constraints on negative impedances could exist in specific optimization analysis, which will be discussed additionally. Finally, recalling the research works on piezoelectric shunt damping [16, 19], a similarity between both damping techniques can be underlined that the stability of electromechanical system is related to the ratio between the inherent electric features of transducer and electric parameters of shunt.

In the following, closed-form solutions will be derived to optimum designs of EMSDs based on three aforementioned optimization criteria: fixed points theory, $H_2$ optimization criterion and maximum damping criterion.

### *3.2. Optimum design based on fixed points theory*

In this subsection, the coupled system is subjected to harmonic force excitation and the optimum design is conducted according to the fixed points theory proposed by Den Hartog [2]. The optimal frequency tuning ratio $\phi$ is firstly defined, with which the magnitudes at the two invariant points are equalized. The two fixed points locate at frequencies where the frequency response amplitude of primary structure is independent of the electrical damping $\xi_e$. Considering now two extreme cases where no electrical damping is present (namely $\xi_e \to 0$) and where the electromagnetic coil is open-circuited (namely $\xi_e \to \infty$), the corresponding squared magnitudes of FRF can be then simplified as:

$$\mathrm{H}^2_{\xi_e\to 0} = \frac{(1+\gamma)^2(\phi^2-\alpha^2)^2}{\left[(1+\gamma)(\phi^2-\alpha^2)(1-\alpha^2)-\theta^2\alpha^2\right]^2}, \quad \mathrm{H}^2_{\xi_e\to\infty} = \frac{1}{(1-\alpha^2)^2}. \tag{14}$$

Equating the previous magnitudes yields a quadratic expression in $\alpha^2$ such that

$$\alpha^4 - \left(1+\phi^2+\frac{\theta^2}{2(1+\gamma)}\right)\alpha^2 + \phi^2 = 0 \tag{15}$$

from which one can realize that the two squared frequencies at fixed points satisfy:

$$\alpha^2_{\mathrm{fpt},1} + \alpha^2_{\mathrm{fpt},2} = 1+\phi^2+\frac{\theta^2}{2(1+\gamma)} \tag{16}$$

In addition, the magnitudes should be equal at the fixed points, i.e.

$$\frac{1}{(1-\alpha^2_{\mathrm{fpt},1})^2} = \frac{1}{(1-\alpha^2_{\mathrm{fpt},2})^2} \tag{17}$$

which yields the optimal frequency tuning ratio $\phi_{\mathrm{fpt}}$ and the maximum magnitude of FRF according to the fixed points theory, to be respectively:

$$\phi^2_{\mathrm{fpt}} = 1-\frac{\theta^2}{2(1+\gamma)}, \quad \mathrm{H}\Big|_{\alpha=\alpha_{\mathrm{fpt}},\phi=\phi_{\mathrm{fpt}}} = \frac{\sqrt{2(1+\gamma)}}{\theta}. \tag{18}$$

and the two equal peak magnitudes of FRF locate at:

$$\alpha^2_{\mathrm{fpt},1} = 1-\frac{\theta}{\sqrt{2(1+\gamma)}}, \quad \alpha^2_{\mathrm{fpt},2} = 1+\frac{\theta}{\sqrt{2(1+\gamma)}}. \tag{19}$$

In order to have a non-negative $\phi^2_{\mathrm{fpt}}$, the following constraint should be satisfied for the inductance ratio $\gamma$:

$$\gamma_{\mathrm{fpt}} \geq \frac{\theta^2}{2}-1 \tag{20}$$

In the following, the optimal resistance ratio $\beta$ is determined in such a way that the magnitudes at the two fixed points are global maximum, namely the frequency response curve passes the two fixed points with horizontal tangent. Thus, an another optimal condition is formulated as:

$$\left.\frac{\partial \mathrm{H}^2}{\partial \alpha}\right|_{\alpha=\alpha_{\mathrm{opt}},\beta=\beta_{\mathrm{opt}}} = \frac{1}{\mathrm{D}^2}\left(\frac{\partial \mathrm{N}}{\partial \alpha}\cdot \mathrm{D} - \mathrm{N}\cdot\frac{\partial \mathrm{D}}{\partial \alpha}\right) = 0 \tag{21}$$

where N and D stand for the numerator and denominator polynomials of squared magnitude function of FRF, which are given by

$$\begin{aligned} \mathrm{N}(\alpha) &= (1+\gamma)^2(\phi^2-\alpha^2)^2 + \alpha^2\kappa^2(1+\beta)^2 \\ \mathrm{D}(\alpha) &= [(1+\gamma)(1-\alpha^2)(\phi^2-\alpha^2) - \theta^2\alpha^2]^2 + \alpha^2\kappa^2(1+\beta)^2(1-\alpha^2)^2 \end{aligned} \tag{22}$$

By substituting Eq. (22) into Eq. (21) and solving the ordinary differential equation, the optimal resistance ratios obtained at each fixed point, $\alpha_{\mathrm{fpt},1}$ or $\alpha_{\mathrm{fpt},2}$, are slightly different with each other:

$$\beta_{\mathrm{fpt},1} = \frac{\theta\sqrt{1+\gamma}}{2\kappa}\sqrt{6-\sqrt{\frac{2}{1+\gamma}}\theta} - 1, \quad \beta_{\mathrm{fpt},2} = \frac{\theta\sqrt{1+\gamma}}{2\kappa}\sqrt{6+\sqrt{\frac{2}{1+\gamma}}\theta} - 1. \tag{23}$$

which is rational in that the two fixed points can not be local maximum simultaneously. As proposed in Ref. [2], the optimal electrical damping $\xi_{\mathrm{e,fpt}}$ of the resonant shunt damper is defined as the root mean square value of electrical damping ratios calculated at two invariant points by using Eq. (6). Therefore, the optimal resistance ratio $\beta_{\mathrm{fpt}}$ can be eventually calculated in such a way that:

$$\beta_{\mathrm{fpt}} = \sqrt{\frac{(\beta_{\mathrm{fpt},1}+1)^2 + (\beta_{\mathrm{fpt},2}+1)^2}{2}} - 1 = \frac{\theta}{\kappa}\sqrt{\frac{3}{2}(1+\gamma)} - 1 \tag{24}$$

The authors remark that our global expressions of optimal frequency tuning ratio (18) and optimal resistance ratio (24) are consistent with the study reported in Ref. [25] when no additional inductance is included in the shunt circuit ($\gamma = 0$).

By considering the general stability condition (13) and Eq. (20), one can find that in the optimal damping scenario based on the fixed points theory, the inductance ratio $\gamma$ should be bounded by

$$\gamma \geq \gamma_{\mathrm{cri,fpt}} = \frac{\theta^2}{2} - 1 \tag{25}$$

One can easily notice from Eq. (18) that the peak magnitude of FRF increases monotonically with inductance ratio $\gamma$. Therefore, the best achievable damping performance of a RLC series shunt is attained when $\gamma$ is tuned at the critical value. At this specific value $\gamma_{\mathrm{cri,fpt}}$, we have

$$\beta_{\mathrm{cri,fpt}} = \frac{\sqrt{3}\theta^2}{2\kappa} - 1, \quad \phi_{\mathrm{cri,fpt}} = 0, \quad \mathrm{H}_{\mathrm{cri,fpt}} = 1. \tag{26}$$

from which we conclude that the critical damping performance of a RLC shunt is observed at the occasion of electrical resonance being vanished.

Reminding the similarity between classic DVAs and EMSDs, one can define the equivalent "mass" ratio $\mu$ for EMSDs in such a way [34]

$$\mu = \frac{k_e^2 C}{M_s} = \frac{\theta^2}{(1+\gamma)\phi^2} \tag{27}$$

In the optimal scenario relevant to fixed points theory, the equivalent mass ratio $\mu$ can be expressed in terms of inductance ratio $\gamma$ and electromagnetic coupling coefficient $\theta$ by substituting Eq. (18) into Eq. (27), yielding

$$\mu_{\mathrm{fpt}} = \frac{\theta^2}{1+\gamma-\dfrac{\theta^2}{2}} \tag{28}$$

One can conclude that a negative inductance ($\gamma < 0$) will result in a greater equivalent mass ratio leading to a better performance of vibration attenuation, as observed for classic DVAs. When the inductance ratio $\gamma$ is tuned fairly close to its lower bound $\gamma_{\mathrm{cri,fpt}}$, the equivalent mass ratio $\mu_{\mathrm{fpt}}$ tends to infinity and the EMSDs will reach its ultimate attenuation performance. Therefore, the advantage claimed for EMSDs over DVAs resides in the fact that the equivalent mass ratio can go up to infinity by using negative impedance in the shunt circuit, while it is impossible for DVAs in light of physical restrictions, such as mass, volume etc.

### *3.3. Optimum design based on $H_2$ optimization criterion*

In this subsection, the electromechanical system is considered to be randomly excited. Since the input cannot be characterized by a single harmonic frequency, the $H_2$ optimization criterion should be thus employed to minimize the total vibration energy over the whole range of frequency, namely the area covered by the frequency response curve of the main system.

Assuming that the excitation force has a constant power spectral density (PSD) $S_f$ over the whole range of frequency, we can then define a performance index $I$ as:

$$I = \frac{E[x^2]}{2\pi S_f \omega_s / K_s^2} \tag{29}$$

where $E[\cdot]$ denotes the mean square value. And $E[x^2]$ can be evaluated by the following expression:

$$E[x^2] = \int_{-\infty}^{+\infty} \left|\frac{X}{F}\right|^2 S_f d\omega = \frac{S_f \omega_s}{K_s^2} \int_{-\infty}^{+\infty} \left|\frac{X}{F/K_s}\right|^2 d\alpha = \frac{S_f \omega_s}{K_s^2} \int_{-\infty}^{+\infty} \mathrm{H}^2(\alpha) d\alpha \tag{30}$$

The infinite integral in Eq. (30) can be evaluated by applying the residue theorem [35]. An analytical form of result for this integral is also provided in this paper. For a rational function $\mathrm{G}(\alpha)$ having the form of

$$\mathrm{G}(\alpha) = \frac{b_0 + b_1(j\alpha)^1 + b_2(j\alpha)^2 + b_3(j\alpha)^3}{a_0 + a_1(j\alpha)^1 + a_2(j\alpha)^2 + a_3(j\alpha)^3 + a_4(j\alpha)^4} \tag{31}$$

its corresponding integral over the infinite range of frequencies can be evaluated by the following closed-form formula [36]:

$$\int_{-\infty}^{+\infty} \left|\mathrm{G}(\alpha)\right|^2 d\alpha = \pi \frac{\dfrac{b_0^2\,(a_2 a_3 - a_1 a_4)}{a_0} + a_3\left(b_1^2 - 2b_0 b_2\right) + a_1\left(b_2^2 - 2b_1 b_3\right) + \dfrac{b_3^2\,(a_1 a_2 - a_0 a_3)}{a_4}}{a_1\,(a_2 a_3 - a_1 a_4) - a_0 a_3^2} \tag{32}$$

By comparing Eqs. (7) and (31), the coefficients may be written as:

$$\begin{aligned} &b_0 = (1+\gamma)\phi^2, \quad b_1 = (1+\beta)\kappa, \quad b_2 = 1+\gamma, && b_3 = 0, \\ &a_0 = (1+\gamma)\phi^2, \quad a_1 = (1+\beta)\kappa, \quad a_2 = (1+\gamma)(1+\phi^2)+\theta^2, \quad a_3 = (1+\beta)\kappa, \quad a_4 = 1+\gamma. \end{aligned} \tag{33}$$

Mathematically speaking, the global minimum of $I(\beta, \phi, \gamma)$ is attained at points satisfying the following conditions:

$$\frac{\partial I}{\partial \beta} = 0, \quad \frac{\partial I}{\partial \phi} = 0, \quad \frac{\partial I}{\partial \gamma} = 0. \tag{34}$$

However, the authors notice that such a global extreme of $I(\beta, \phi, \gamma)$ does not exist. Hence, a trade-off is made and the optimization is only conducted with regard to resistance ratio $\beta$ and frequency tuning ratio $\phi$, i.e.

$$\frac{\partial I}{\partial \beta} = 0, \quad \frac{\partial I}{\partial \phi} = 0. \tag{35}$$

from which the optimal values of $\beta$ and $\phi$ can be obtained as a function of inductance ratio $\gamma$, respectively

$$\begin{aligned}\phi_{\mathrm{h2}}^2 &= 1 - \frac{\theta^2}{2(1+\gamma)} \\ \beta_{\mathrm{h2}} &= \frac{\theta}{\kappa}\sqrt{1+\gamma-\frac{\theta^2}{4}} - 1\end{aligned} \tag{36}$$

The non-negativity constraint on $\phi_{\mathrm{h2}}^2$ imposes that $\gamma \geq \theta^2/2 - 1$, and the general stability condition $\beta > -1$ leads to $\gamma > \theta^2/4 - 1$. Therefore, the aforementioned optimal formulae (36) will not have physical meaning except if the inductance ratio $\gamma$ satisfies the following constraint

$$\gamma \geq \gamma_{\mathrm{cri,h2}} = \frac{\theta^2}{2} - 1 \tag{37}$$

It is noted that this boundary value resides in the stable region, the critical attenuation performance of a series RLC shunt under random vibration is then achieved at $\gamma = \gamma_{\mathrm{cri,h2}}$, at which we have

$$\beta_{\mathrm{cri,h2}} = \frac{\theta^2}{2\kappa} - 1, \quad \phi_{\mathrm{cri,h2}} = 0. \tag{38}$$

### *3.4. Optimum design based on maximum damping criterion*

In this subsection, the coupled system is expected to experience short-term excitation. In the objective of suppressing transient vibration response and accelerating its decay, the optimum design should be conducted according to the maximum damping criterion. Before applying this calibration strategy, some basic features of maximum damping criterion will be first presented.

In this study, the electromechanical system has two state variables, $x$ and $y$ in mechanical and electrical domains, respectively. Therefore, its corresponding characteristic polynomial is of order 4 and thus 4 roots can be obtained. Supposing that the transient response $x(\tau)$ can be described by the following form:

$$x(\tau) = A_1 e^{\lambda_1 \tau} + A_2 e^{\lambda_2 \tau} + A_3 e^{\lambda_3 \tau} + A_4 e^{\lambda_4 \tau} \tag{39}$$

where $A_1$, $A_2$, $A_3$ and $A_4$ are polynomials in terms of dimensionless time $\tau$, which depends on the initial states of system, and $\lambda_1$, $\lambda_2$, $\lambda_3$ and $\lambda_4$ stand for the eigenvalues of characteristic equation relevant to the dimensionless system. The transient response should be eventually decayed to zero so that all eigenvalues should locate at the left-half complex plane. And the decay rate is characterized by its time constants, which are the inverse of real parts of eigenvalues. Moreover, the lower the time constants, the faster the transient response will be suppressed. Thus, the performance index to be maximized in this calibration can be chosen as:

$$\Lambda = -\max_i \left\{ \mathrm{Re}(\lambda_i) \right\} \tag{40}$$

Hence, the maximum damping criterion aims at maximizing the absolute value of the real part of the rightmost eigenvalue, namely all eigenvalues should locate as far as possible away from the imaginary axis.

As stated in the literature [7, 8], the maximum damping is attained when the eigenvalues of system take the form of a double pair of complex conjugates. Supposing that the four roots are expressed as: $\lambda_1 = \lambda_3 = -p + jq$ and $\lambda_2 = \lambda_4 = -p - jq$, with $p$ being positive, the corresponding characteristic polynomial can be then factorized and further formulated in terms of its four roots

$$(\lambda - \lambda_1) \cdot (\lambda - \lambda_2) \cdot (\lambda - \lambda_3) \cdot (\lambda - \lambda_4) = 0 \tag{41}$$

which can be expanded and rewritten in the polynomial form of $\lambda$ as

$$\lambda^4 + 4p\lambda^3 + (4p^2 + 2r^2)\lambda^2 + 4pr^2\lambda + r^4 = 0 \tag{42}$$

with $r^2 = p^2 + q^2$ denoting the squared magnitude of roots.

By comparing coefficients in expressions (11) and (42), four equations can be obtained as follows:

$$4p = \frac{\kappa(1+\beta)}{1+\gamma} \tag{43a}$$

$$4p^2 + 2r^2 = 1 + \phi^2 + \frac{\theta^2}{1+\gamma} \tag{43b}$$

$$4pr^2 = \frac{\kappa(1+\beta)}{1+\gamma} \tag{43c}$$

$$r^4 = \phi^2 \tag{43d}$$

Combining Eqs. (43a) and (43c) yields $r = 1$, hence, one has $\phi = r^2 = 1$ according to Eq. (43d). With the knowledge of $r$ and $\phi$, one can determine the optimal $\beta$ by substituting Eq. (43a) into Eq. (43b). Finally, the optimal parameters tuned by maximum damping criterion can be described in terms of inductance ratio $\gamma$ as

$$\beta_{\mathrm{mdc}} = \frac{2\theta}{\kappa}\sqrt{1+\gamma} - 1, \quad \phi_{\mathrm{mdc}} = 1, \quad p = \frac{\theta}{2\sqrt{1+\gamma}}, \quad r = 1. \tag{44}$$

The inequality $p^2 \le r^2$ imposes that $\gamma \ge \theta^2/4 - 1$. Therefore, the inductance ratio $\gamma$ for the optimal configuration based on maximum damping criterion should be constrained by

$$\gamma \ge \gamma_{\mathrm{cri,mdc}} = \frac{\theta^2}{4} - 1 \tag{45}$$

At this very critical value, the optimal parameters (44) are reduced to

$$\beta_{\mathrm{cri,mdc}} = \frac{\theta^2}{\kappa} - 1, \quad \phi_{\mathrm{cri,mdc}} = 1, \quad p_{\mathrm{cri,mdc}} = 1. \tag{46}$$

which designates that all the roots locate on the real axis of complex plane with their abscissa being $-1$.

### *3.5. Summary and discussion*

Up to now, all optimal parameters of resonant EMSD are analytically derived according to three different tuning rules, as summarized in Table 1. The optimal resistance ratio $\beta_{\mathrm{opt}}$ and optimal frequency tuning ratio $\phi^2_{\mathrm{opt}}$ are given as a function of the inductance ratio $\gamma$ whose lower bound is also specified in each case. It is remarkable that the resistance and inductance ratios, $\beta$ and $\gamma$, lie inside the stability region, and the need of negative impedances is of the same order of magnitude as that of electromagnetic transducer, which is feasible in practical applications.

Given that the electromechanical coupling coefficient $\theta$ is usually small, it is observable from Table 1 that a negative resistance and/or a negative inductance could be involved in the shunt circuit. Negative resistances and inductances do not exist physically, and could be implemented by means of negative impedance converters [37].

Before going through the numerical analysis, the analytical solutions in this present paper should be compared to existing solutions in the literature in order to verify the correctness of proposed study. Generally, an EMSD is characterized by two tuning parameters: electrical damping ratio $\xi_{\mathrm{e}}$ and frequency tuning ratio $\phi$. In this work, the optimal electrical damping ratio $\xi_{\mathrm{e,opt}}$ can be evaluated by using Eq. (6) with the knowledge

| | **Fixed points theory** | $H_2$ **optimization** | **Maximum damping** |
|---|---|---|---|
| $\gamma$ | $\left[\frac{\theta^2}{2}-1,\,+\infty\right)$ | $\left[\frac{\theta^2}{2}-1,\,+\infty\right)$ | $\left[\frac{\theta^2}{4}-1,\,+\infty\right)$ |
| $\beta_{\text{opt}}$ | $\frac{\theta}{\kappa}\sqrt{\frac{3}{2}(1+\gamma)}-1$ | $\frac{\theta}{\kappa}\sqrt{1+\gamma-\frac{\theta^2}{4}}-1$ | $\frac{2\theta}{\kappa}\sqrt{1+\gamma}-1$ |
| $\phi^2_{\text{opt}}$ | $1-\frac{\theta^2}{2(1+\gamma)}$ | $1-\frac{\theta^2}{2(1+\gamma)}$ | $1$ |

Table 1: Optimal parameters of an EMSD connected with a RLC series shunt circuit based on different optimization criteria.

| **Criterion** | **This paper** | **Ref. [25]** | **Ref. [26]** |
|---|---|---|---|
| FPT | $\xi_{\text{e}}=\sqrt{\frac{3}{8(1+\gamma)}}\theta$<br>$\phi=\sqrt{1-\frac{\theta^2}{2(1+\gamma)}}$ | $\xi_{\text{e}}=\sqrt{\frac{3}{8}}\theta$<br>$\phi=\sqrt{1-\frac{\theta^2}{2}}$ | |
| $H_2$ | $\xi_{\text{e}}=\sqrt{\frac{\theta^2}{4(1+\gamma)}-\frac{\theta^4}{16(1+\gamma)^2}}$<br>$\phi=\sqrt{1-\frac{\theta^2}{2(1+\gamma)}}$ | | $\xi_{\text{e}}=\sqrt{\frac{\theta^2}{4}-\frac{\theta^4}{16}}$<br>$\phi=\sqrt{1-\frac{\theta^2}{2}}$ |

Table 2: Comparison of optimal parameters with existing literature.

of optimal resistance ratio $\beta_{\text{opt}}$, as listed in Table 1. It is worth noting that this present paper proposed a systematic study on optimization of resonant EMSDs under various excitation scenarios, and to the best of our knowledge, MDC-based optimum design had not been conducted before. For this reason, only optimal solutions relevant to FPT and $H_2$ optimization criterion are compared to current references. In Table 2 is presented a comparison of optimal tuning parameters of resonant EMSDs developed in this paper and from the current literature. It is remarkable from Table 2 that when no additional inductance is included in the shunt circuit, namely $\gamma = 0$ and a RC shunt is employed instead of a RLC shunt, the optimal solutions in this paper are exactly the same as the ones in Ref. [25] when tuning the EMSD according to the fixed points theory, and are consistent with the results in Ref. [26] in terms of $H_2$ optimum design. Hence, a conclusion can be drawn that the proposed analytical solutions are correct and can be applied in any further study. Finally, the influence of an additional inductance on the shunt performance will be underlined in the following numerical investigation.

## 4. Numerical investigation

In this section, the performance of resonant EMSDs with different optimization criteria will be examined under various excitation circumstances and we will discuss the contribution of negative inductance to frequency response magnitude and shunt damping capability. The following study is carried out for the model investigated in Ref. [23], whose physical properties are listed in Table 3.

### *4.1. Harmonic excitation scenario*

Figure 3 depicts the frequency response of primary structure with optimal parameters relevant to the fixed points theory against the normalized excitation frequency $\alpha$ and the inductance ratio $\gamma$ under harmonic excitation. The squared magnitude of FRF, $\text{H}^2(\alpha,\gamma)$, is drawn in logarithmic scale. It is noticeable that compared to the

| **Parameter** | $M_s$ | $K_s$ | $R_i$ | $L_i$ | $k_e$ |
|---|---|---|---|---|---|
| **Value** | 0.15 | 56 | 3.3 | 1 | 3.4 |
| **Unit** | kg | $\mathrm{kN\,m^{-1}}$ | Ω | mH | $\mathrm{N\,A^{-1}}$ |

Table 3: Physical parameters of an EMSD extracted from Ref. [23].

RC series shunt in Ref. [25] (curve C1 in Fig. 3, $\gamma = 0$), the inclusion of a negative inductance ($\gamma < 0$) in the shunt circuit leads to a decrease of peak magnitudes (see also Eq. (18)) and a spreading of fixed points (the two curves C3 and C4 separate from each other, see also Eq. (19)). In other words, increasing the magnitude of negative inductance results in a more flat and smaller frequency response of the main system, broadening the absorbing area where vibration magnitude is reduced. When the inductance ratio $\gamma$ is tuned at the critical value $\gamma_{\mathrm{cri,fpt}}$ (curve C2 in Fig. 3), the left invariant point will diminish to 0, namely the scenario of static force excitation, thus the peak magnitude is reduced to that of static displacement of main system.

Frequency responses of the main system with different optimum designs are plotted in Fig. 4 with $\gamma = 0$ (namely RC series shunt in Ref. [25]) and $\gamma = -0.5$ (namely RLC series shunt) under harmonic disturbance. It is noticed that in both cases, no flat plateau is present and an evident resonant peak exists in the mechanical frequency response relevant to the maximum damping technique. It is reasonable due to the fact that this technique is oriented towards transient vibration suppression instead of improving the steady state response. Nevertheless, both the fixed point theory and $H_2$ optimization criterion are based on the optimization of frequency response of primary structure, hence the peak at resonance is cancelled, two lower peaks appear and the frequency response curve becomes more flat. By applying a RC shunt circuit, as shown in Fig. 4a, the maximum magnitude of the main system decreases from 28.6dB (short circuit) to 9.9dB (FPT), 10.1dB ($H_2$) and 13dB (MDC). The inclusion of negative inductance adds an attenuation of 3dB compared to the RC series shunt for all three calibrations. Finally, one can state that the fixed point theory leads to the best performance in terms of confining the $H_\infty$ norm of frequency response under harmonic excitation.

However, both optimization techniques other than maximum damping criterion aim at improving steady state response, for which the damping capability of shunt circuit is not optimized and thereby the energy dissipation linked to optimal electrical damping $\xi_{\mathrm{e,opt}}$ is not maximized. $\xi_{\mathrm{e,opt}}$ can be calculated by using Eq. (6) with the optimal parameters listed in Table 1. As depicted in Fig. 5, the shunt circuit optimized by the maximum damping criterion possesses the largest electrical damping over the whole range of inductance ratio $\gamma$. And the shunt circuit calibrated by the $H_2$ optimization criterion always underperforms its other two counterparts in terms of electrical damping, namely dissipated energy. Besides, the optimal electrical damping ratios $\xi_{\mathrm{e,opt}}$ always decreases as the magnitude of negative inductance reduces. As $\gamma$ increases from $\gamma_{\mathrm{cri,fpt}}$ to 0 (namely the case of a RC series shunt in Ref. [25]), a reduction of 67.9% in $\xi_{\mathrm{e,opt}}$ is observed for the EMSD relevant to maximum damping criterion.

### *4.2. Random excitation scenario*

Fig. 6 demonstrates the fluctuation of optimal performance indices $I_{\mathrm{opt}}$ as a function of inductance ratio $\gamma$. The $H_2$-based shunt damper has the smallest performance index over the whole range of $\gamma$, which designates that the relevant system vibrates the least. One can also notice that the fixed points theory leads to performance

fairly close to the $H_2$ optimization criterion, while the MDC-based shunt damper has the worst performance under random vibration.

An analysis in the temporal domain is also conducted to investigate the dynamics responses of EMSDs under random force excitation. The PSD of external force $S_f$ is set as $10\mathrm{N}^2 \cdot \mathrm{Hz}^{-1}$ and the inductance ratio is imposed at $\gamma = -0.5$. In this scenario, the equations of motion (3) become actually a set of stochastic differential equations (SDE), and the Euler-Maruyama scheme [38] is adopted to solve the SDEs numerically. The iteration step is fixed at $10^{-4}$s and four simulations are performed with different system parameters, as shown in Fig. 7. In order to characterize these random time histories, the root mean square value (RMS) is employed, which are calculated as: (a) 13.3mm; (b) 4.3mm; (c) 4.2mm; (d) 4.9mm. In contrast to the short-circuited case, FPT-, $H_2$- and MDC-based EMSDs with RLC series shunt demonstrate the capability of reducing the RMS displacement of mechanical system by 67.7%, 68.4% and 63.2%, respectively, while they outperform their counterparts with RC series shunt (i.e. $\gamma = 0$) by 17.3%, 17.7% and 15.5%, respectively. It is then hinted that the $H_2$-based EMSD has the best performance under broadband random vibration (lowest RMS value) and the order of performance is exactly the same as the one predicted by the performance index $I_{\mathrm{opt}}$ in the previous study.

### *4.3. Transient excitation scenario*

The damping performance of transient vibration is now investigated. As described in previous section, the exponential decay rate of vibration for a shunt circuit is quantified by the performance index $\Lambda$. Fig. 8a shows the evolution of optimal performance indices $\Lambda_{\mathrm{opt}}$ relevant to each calibration strategy against the inductance ratio $\gamma$. It is noticeable that the maximum damping criterion always has the largest performance index over the whole range of inductance ratio $\gamma$, while that of $H_2$ optimization criterion is always the smallest. It is hinted that the maximum damping calibration yields the best decay rate of transient response due to short-termed disturbance. In Fig. 8b, eigenvalues related to different criteria are located in the complex plane with inductance ratio being $\gamma = -0.5$. The coupled system has two pairs of conjugate roots when calibrated by the fixed point theory and $H_2$ optimization criterion, while the two pairs of conjugate roots coalesce into a double pair of conjugate roots for the maximum damping strategy and the absolute value of real parts of its roots is the largest. The performance indices for three calibration procedures can be read directly as: $\Lambda_{\mathrm{fpt}} = 0.186$, $\Lambda_{h2} = 0.137$, $\Lambda_{\mathrm{mdc}} = 0.321$.

A numerical simulation is finally performed to investigate the transient vibration response of the EMSD. In this study, the EMSD is supposed to undergo vibration freely, i.e. $f(t) = 0$, and an initial displacement condition is imposed instead. The transient response of system can be then obtained by solving the dimensionless ordinary differential equations (5) with the ode45 solver built in Matlab. The initial states are set as: $x(0) = x_0 = 1$ and $x'(0) = y(0) = y'(0) = 0$. In Figs. 9a and 9b, the transient responses of normalized displacement and absolute acceleration are plotted when the EMSD is short-circuited (as marked by dotted line) or calibrated according to three optimization criteria with negative inductance ratio being $\gamma = \gamma_{\mathrm{cri,fpt}} = \gamma_{\mathrm{cri,h2}}$. It is observable that all calibration techniques contribute to attenuate the transient response significantly, compared to the short-circuited scenario. Fig. 9b shows that the acceleration response related to maximum damping criterion decays to zero more quickly than other two methods, while it leads to a relatively large displacement response. Another simulation of MDC-based EMSDs is performed at $\gamma = 0$ (i.e. RC series shunt) and $\gamma_{\mathrm{cri,mdc}}$ (i.e. RLC series shunt), as plotted in Figs. 9c and 9d. Compared to the RC series shunt, the RLC series shunt with negative inductance can eliminate the disturbance and decay to zero in much shorter time. Besides, one can note that

all its eigenvalues coincide and locate at $(-1, 0)$ in the complex plane when the inductance ratio $\gamma$ arrives at the critical value $\gamma_{\text{cri,mdc}}$, therefore, its utmost performance index is equal to unity, i.e. $\Lambda_{\text{cri,mdc}} = 1$.

### *4.4. Discussion*

To this end, it is pertinent to investigate the applicability of current optimum designs, which are conducted under the assumption of undamped primary system, to lightly damped mechanical systems. In Fig. 10a is depicted the comparison of frequency responses of undamped primary system (marked by solid line) and the one with 1% viscous damping (marked by dash-dotted line). The EMSD is calibrated by fixed points theory with negative inductance ratio being $\gamma = 0$. It is suggested that the neglect of inherent damping of primary system will lead to an overestimation of 3.7% on the peak vibration amplitude of primary system, which is negligible in practical applications. Besides, the presence of inherent damping leads to a slight misalignment between two resonance peaks. In Fig. 10b is demonstrated the peak vibration amplitude difference of damped primary system compared to the one corresponding to undamped mechanical system as a function of viscous damping $\xi$. It is apparent that the difference increases monotonically as the inherent damping of primary system increases. One can thus draw a conclusion that the aforementioned optimum design for undamped primary system can be employed in the case where the mechanical system is lightly damped.

## 5. Conclusions

This paper investigates an undamped system coupled with a resonant EMSD, and its optimum designs are carried out according to three different optimization strategies, each of which is appropriate for a specific excitation circumstance. The optimal parameters are derived analytically and are formulated as a function of the inductance ratio $\gamma$. Lower bounds of inductance ratio $\gamma$ in the stable region are also provided for all three strategies. By comparing to the current literature, it is demonstrated that a negative inductance in series connection with a RC shunt circuit will always result in reducing the peak magnitude of frequency response of primary structure, increasing the absorbing frequency bandwidth and thus enhancing the damping performance. For instance, the FPT-based resonant EMSDs can reduce the peak magnitude of primary system to the level of static displacement when the negative inductance is tuned to the corresponding lower bound.

A detailed numerical investigation is performed, which compares the performance of resonant EMSDs with different tuning rules under various types of disturbance. The fixed points theory and $H_2$ optimization criterion are more appropriate in terms of improving the steady state response, for which damping capability towards target vibration mode is not optimized. While the maximum damping criterion is oriented towards increasing the damping, and thereby accelerating the energy dissipation. Numerical results prove that the maximum damping criterion can lead to the superior exponential decay rate.

In this paper, the close-form solution to the $H_\infty$ optimization problem of EMSDs connected with a RLC series shunt circuit is obtained by using the fixed points theory, which designates that the solution provided is merely approximative. Future works could be dedicated to the derivation of exact solutions to the $H_\infty$ optimization problem.

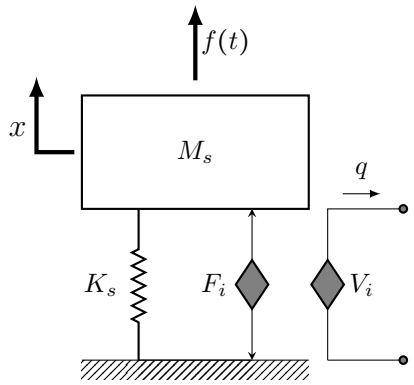


Figure 1: A SDOF undamped primary structure coupled with an EMSD under force excitation.

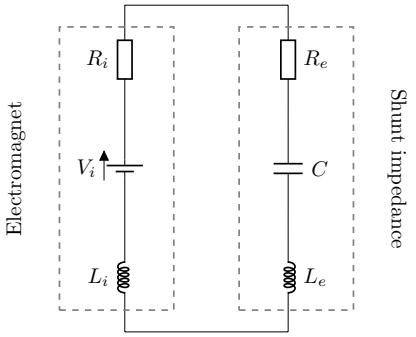


Figure 2: Electrical model of electromagnetic transducer connected with a RLC series shunt circuit.

## References


[1] J. Q. Sun, M. R. Jolly, M. A. Norris, Passive, adaptive and active tuned vibration absorbers- a survey, Journal of Vibration and Acoustics, Transactions of the ASME 117 (1995) 234–242. doi:10.1115/1.2836462.

[2] J. P. Den Hartog, Mechanical vibrations, Courier Corporation, 1985.

[3] O. Nishihara, T. Asami, Closed-form solutions to the exact optimizations of dynamic vibration absorbers (minimizations of the maximum amplitude magnification factors), Journal of Vibration and Acoustics, Transactions of the ASME 124 (4) (2002) 576–582. doi:10.1115/1.1500335.

[4] O. F. Tigli, Optimum vibration absorber (tuned mass damper) design for linear damped systems subjected to random loads, Journal of Sound and Vibration 331 (13) (2012) 3035–3049. doi:10.1016/j.jsv.2012.02.017.

[5] T. Asami, T. Wakasono, K. Kameoka, M. Hasegawa, H. Sekiguchi, Optimum design of dynamic absorbers for a system subjected to random excitation, JSME International Journal, Series 3: Vibration, Control Engineering, Engineering for Industry 34 (2) (1991) 218–226. doi:10.1299/jsmec1988.34.218.

[6] T. Asami, O. Nishihara, A. M. Baz, Analytical solutions to $h_\infty$ and $h_2$ optimization of dynamic vibration absorbers attached to damped linear systems, Journal of Vibration and Acoustics, Transactions of the ASME 124 (2) (2002) 284–295. doi:10.1115/1.1456458.

[7] N. W. Hagood, A. von Flotow, Damping of structural vibrations with piezoelectric materials and passive

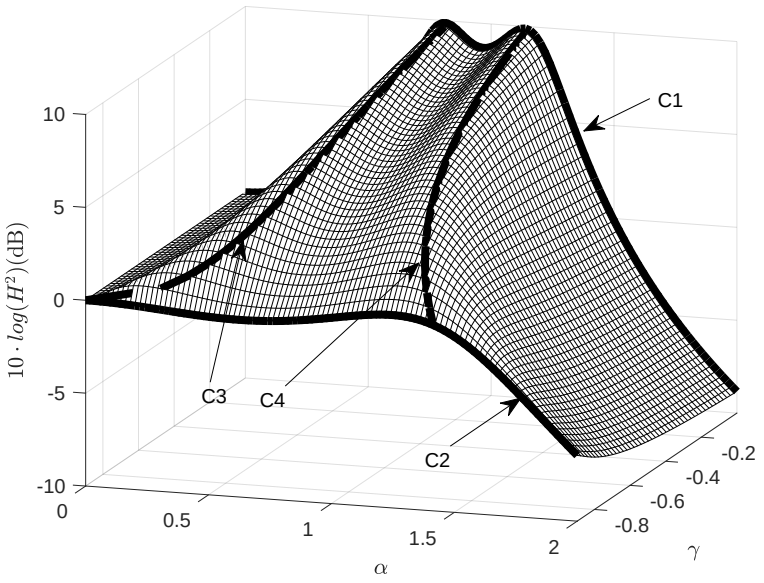


Figure 3: Vibration frequency response of primary system versus normalized excitation frequency $\alpha$ and inductance ratio $\gamma$ with FPT-based optimal parameters under harmonic force excitation. The curve C1 stands for the optimal frequency response with $\gamma = 0$ (namely using a RC series shunt as in Ref. [25]). The curve C2 indicates the critical optimal damping performance by using a RLC series shunt with $\gamma = \gamma_{\mathrm{cri,fpt}}$. The two curves C3 and C4 represent the evolution of vibration magnitudes at two invariant points with respect to $\gamma$.

electrical networks, Journal of Sound and Vibration 146 (2) (1991) 243–268. doi:10.1016/0022-460X(91)90762-9.

[8] G. Caruso, A critical analysis of electric shunt circuits employed in piezoelectric passive vibration damping, Smart Materials and Structures 10 (5) (2001) 1059–1068. doi:10.1088/0964-1726/10/5/322.

[9] P. Xiang, A. Nishitani, Structural vibration control with the implementation of a pendulum-type non traditional tuned mass damper system, JVC/Journal of Vibration and Control 23 (19) (2017) 3128–3146. doi:10.1177/1077546315626821.

[10] P. Soltani, G. Kerschen, G. Tondreau, A. Deraemaeker, Piezoelectric vibration damping using resonant shunt circuits: an exact solution, Smart Materials and Structures 23 (12) (2014) 125014. doi:10.1088/0964-1726/23/12/125014.

[11] S. F. Ali, S. Adhikari, Energy harvesting dynamic vibration absorbers, Journal of Applied Mechanics, Transactions ASME 80 (4) (2013) 041004. doi:10.1115/1.4007967.

[12] D. F. Zhou, C. H. Hansen, J. Li, Suppression of maglev vehicle-girder self-excited vibration using a virtual tuned mass damper, Journal of Sound and Vibration 330 (5) (2011) 883–901. doi:10.1016/j.jsv.2010.09.018.

[13] A. J. Fleming, S. Behrens, S. O. R. Moheimani, Reducing the inductance requirements of piezoelectric shunt damping systems, Smart Materials and Structures 12 (1) (2003) 57–64. doi:10.1088/0964-1726/12/1/307.

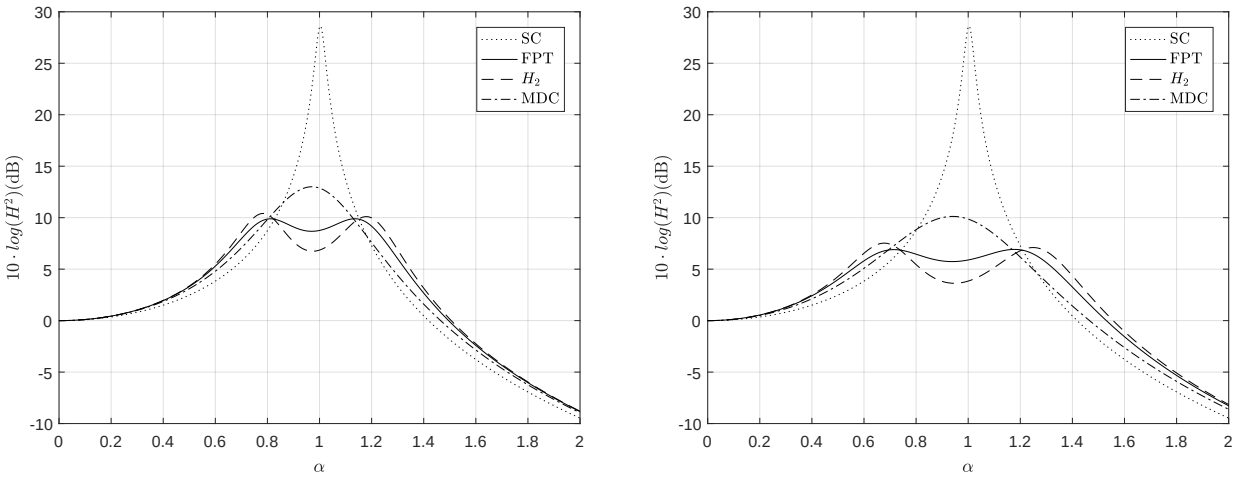


(a) $\gamma = 0$ (b) $\gamma = -0.5$

Figure 4: Mechanical frequency responses of primary structure with optimal parameters relevant to different criteria: (a) $\gamma = 0$ (i.e. RC series shunt in Ref. [25]); (b) $\gamma = -0.5$ (i.e. RLC series shunt). (Dotted line: Short-circuited case (SC), solid: FPT, dashed: $H_2$, dash-dotted: MDC.)


[14] M. Berardengo, S. Manzoni, A. M. Conti, Multi-mode passive piezoelectric shunt damping by means of matrix inequalities, Journal of Sound and Vibration 405 (2017) 287–305. doi:10.1016/j.jsv.2017.06.002.

[15] I. Giorgio, A. Culla, D. Del Vescovo, Multimode vibration control using several piezoelectric transducers shunted with a multiterminal network, Archive of Applied Mechanics 79 (9) (2009) 859–879. doi:10.1007/s00419-008-0258-x.

[16] B. De Marneffe, A. Preumont, Vibration damping with negative capacitance shunts: Theory and experiment, Smart Materials and Structures 17 (3) (2008) 035015. doi:10.1088/0964-1726/17/3/035015.

[17] M. Neubauer, R. Oleskiewicz, K. Popp, T. Krzyzynski, Optimization of damping and absorbing performance of shunted piezo elements utilizing negative capacitance, Journal of Sound and Vibration 298 (1-2) (2006) 84–107. doi:10.1016/j.jsv.2006.04.043.

[18] M. Neubauer, J. Wallaschek, Vibration damping with shunted piezoceramics: Fundamentals and technical applications, Mechanical Systems and Signal Processing 36 (1) (2013) 36–52. doi:10.1016/j.ymssp.2011.05.011.

[19] M. Berardengo, O. Thomas, C. Giraud-Audine, S. Manzoni, Improved resistive shunt by means of negative capacitance: New circuit, performances and multi-mode control, Smart Materials and Structures 25 (7) (2016) 075033. doi:10.1088/0964-1726/25/7/075033.

[20] S. Manzoni, S. Moschini, M. Redaelli, M. Vanali, Vibration attenuation by means of piezoelectric transducer shunted to synthetic negative capacitance, Journal of Sound and Vibration 331 (21) (2012) 4644–4657. doi:10.1016/j.jsv.2012.05.014.

[21] M. Berardengo, O. Thomas, C. Giraud-Audine, S. Manzoni, Improved shunt damping with two nega-

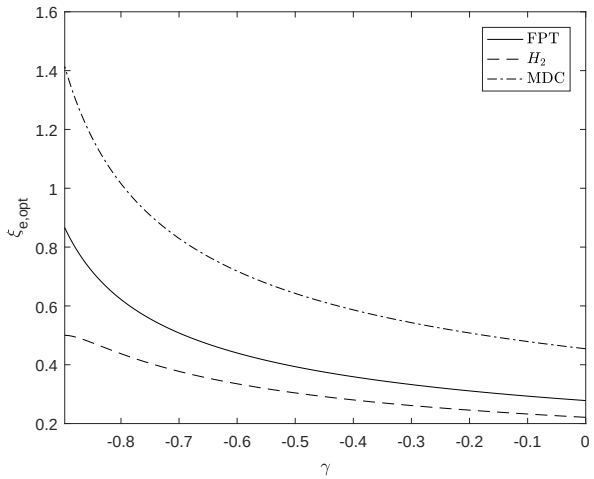


Figure 5: Optimal electrical damping ratio $\xi_{e,opt}$ evaluated by Eq. (6) versus inductance ratio $\gamma$. (Solid line: FPT, dashed: $H_2$, dash-dotted: MDC.)

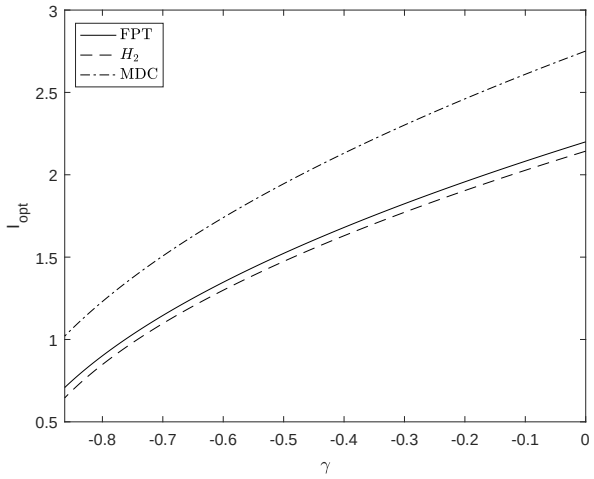


Figure 6: Optimal performance index $I_{opt}$ evaluated by Eq. (29) versus inductance ratio $\gamma$ under random force excitation. (Solid line: FPT, dashed: $H_2$, dash-dotted: MDC.)

tive capacitances: An efficient alternative to resonant shunt, Journal of Intelligent Material Systems and Structures 28 (16) (2017) 2222–2238. doi:10.1177/1045389X16667556.

[22] S. Behrens, A. J. Fleming, S. O. Reza Moheimani, Electromagnetic shunt damping, in: IEEE/ASME International Conference on Advanced Intelligent Mechatronics, AIM, Vol. 2, 2003, pp. 1145–1150. doi:10.1109/AIM.2003.1225504.

[23] S. Behrens, A. J. Fleming, S. O. R. Moheimani, Passive vibration control via electromagnetic shunt damping, IEEE/ASME Transactions on Mechatronics 10 (1) (2005) 118–122. doi:10.1109/TMECH.2004.835341.

[24] D. Niederberger, S. Behrens, A. J. Fleming, S. O. R. Moheimani, M. Morari, Adaptive electromagnetic shunt damping, IEEE/ASME Transactions on Mechatronics 11 (1) (2006) 103–108. doi:10.1109/TMECH.2005.859844.

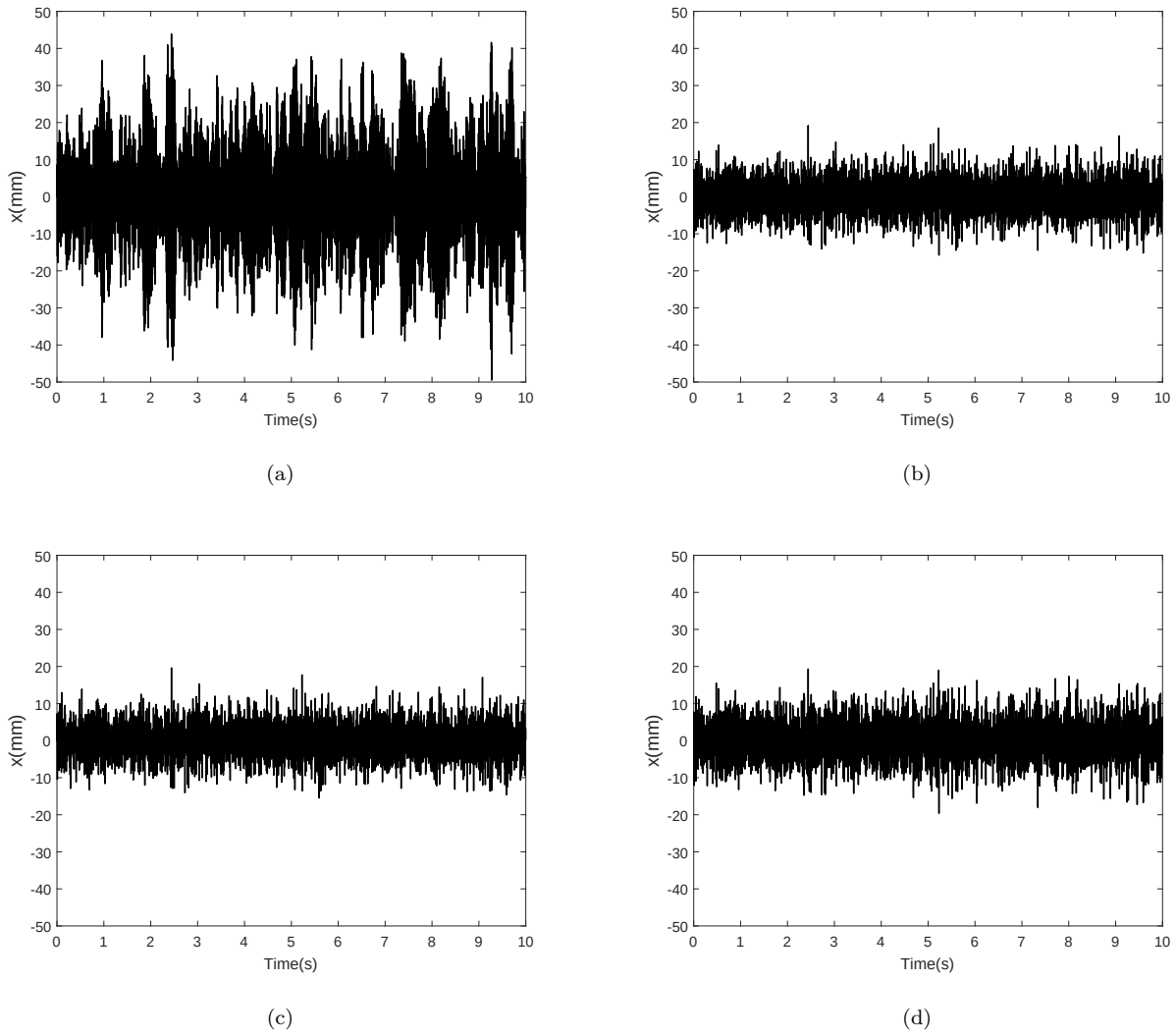


Figure 7: Temporal responses of primary system under random force excitation with $\gamma = -0.5$ and $S_f = 10\mathrm{N}^2 \cdot \mathrm{Hz}^{-1}$: (a) short circuit; (b) FPT; (c) $H_2$; (d) MDC.

[25] T. Inoue, Y. Ishida, M. Sumi, Vibration suppression using electromagnetic resonant shunt damper, Journal of Vibration and Acoustics, Transactions of the ASME 130 (4) (2008) 041003. doi:10.1115/1.2889916.

[26] X. Tang, Y. Liu, W. Cui, L. Zuo, Analytical solutions to $h_2$ and $h_\infty$ optimizations of resonant shunted electromagnetic tuned mass damper and vibration energy harvester, Journal of Vibration and Acoustics, Transactions of the ASME 138 (1) (2016) 011018. doi:10.1115/1.4031823.

[27] H. Niu, X. Zhang, S. Xie, P. Wang, A new electromagnetic shunt damping treatment and vibration control of beam structures, Smart Materials and Structures 18 (4) (2009) 045009. doi:10.1088/0964-1726/18/4/045009.

[28] B. Yan, X. Zhang, H. Niu, Design and test of a novel isolator with negative resistance electromagnetic shunt damping, Smart Materials and Structures 21 (3) (2012) 035003. doi:10.1088/0964-1726/21/3/035003.

[29] X. Zhang, H. Niu, B. Yan, A novel multimode negative inductance negative resistance shunted electromagnetic damping and its application on a cantilever plate, Journal of Sound and Vibration 331 (10) (2012) 2257–2271. doi:10.1016/j.jsv.2011.12.028.

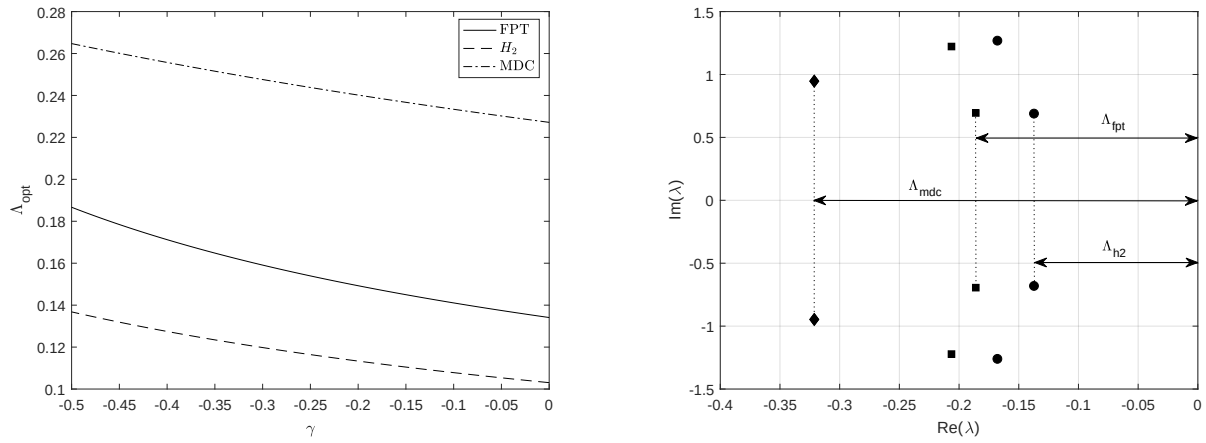


(a) (b)

Figure 8: Root locus of characteristic equations relevant to each calibration technique: (a) Optimal decay performance index $\Lambda_{\text{opt}}$ as a function of inductance ratio $\gamma$ (solid line: FPT, dashed: $H_2$, dash-dotted: MDC); (b) Root location with $\gamma = -0.5$ (square marker: FPT, circle: $H_2$, diamond: MDC).


[30] B. Yan, X. Zhang, Y. Luo, Z. Zhang, S. Xie, Y. Zhang, Negative impedance shunted electromagnetic absorber for broadband absorbing: Experimental investigation, Smart Materials and Structures 23 (12) (2014) 125044. doi:10.1088/0964-1726/23/12/125044.

[31] A. Stabile, G. S. Aglietti, G. Richardson, G. Smet, Design and verification of a negative resistance electromagnetic shunt damper for spacecraft micro-vibration, Journal of Sound and Vibration 386 (2017) 38–49. doi:10.1016/j.jsv.2016.09.024.

[32] A. Stabile, G. S. Aglietti, G. Richardson, G. Smet, A 2-collinear-dof strut with embedded negative-resistance electromagnetic shunt dampers for spacecraft micro-vibration, Smart Materials and Structures 26 (4) (2017) 045031. doi:10.1088/1361-665X/aa61e3.

[33] S. Zhou, C. Jean-Mistral, S. Chesne, Influence of internal electrical losses on optimization of electromagnetic energy harvesting, Smart Materials and Structures 27 (8) (2018) 085015. doi:10.1088/1361-665X/aac8af.

[34] S. Zhu, W. Shen, X. Qian, Dynamic analogy between an electromagnetic shunt damper and a tuned mass damper, Smart Materials and Structures 22 (11) (2013) 115018. doi:10.1088/0964-1726/22/11/115018.

[35] J. Bak, D. J. Newman, Applications of the Residue Theorem to the Evaluation of Integrals and Sums, Springer New York, New York, NY, 2010, pp. 143–160. doi:10.1007/978-1-4419-7288-0_11.

[36] Y. L. Cheung, W. O. Wong, L. Cheng, Optimization of a hybrid vibration absorber for vibration control of structures under random force excitation, Journal of Sound and Vibration 332 (3) (2013) 494–509. doi:10.1016/j.jsv.2012.09.014.

[37] P. Horowitz, W. Hill, The art of electronics, Cambridge Univ. Press, 1989.

[38] S. Zhao, A. Erturk, Electroelastic modeling and experimental validations of piezoelectric energy harvesting from broadband random vibrations of cantilevered bimorphs, Smart Materials and Structures 22 (1) (2013) 015002. doi:10.1088/0964-1726/22/1/015002.

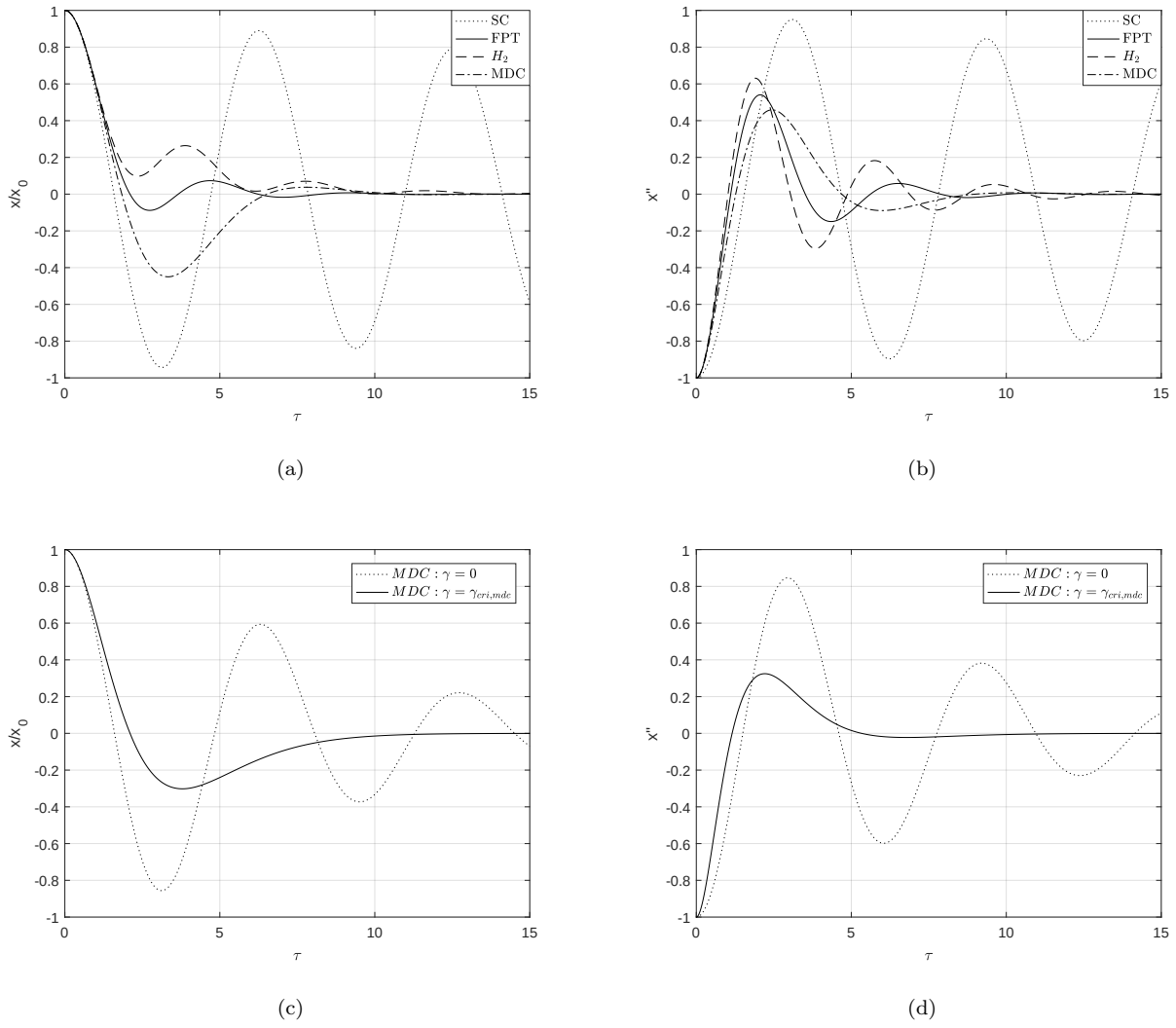


Figure 9: Transient responses under free vibration with initial states as $x(0) = x_0 = 1$ and $x'(0) = y(0) = y'(0) = 0$. (a)(b) normalized displacement response and acceleration time history with $\gamma = \gamma_{\mathrm{cri,fpt}} = \gamma_{\mathrm{cri,h2}}$ (dotted line: SC, solid: FPT, dashed: $H_2$, dash-dotted: MDC). (c)(d) normalized displacement and acceleration time histories relevant to MDC-based EMSD (dotted line: RC series shunt (i.e. $\gamma = 0$), solid: RLC series shunt with $\gamma = \gamma_{\mathrm{cri,mdc}}$).

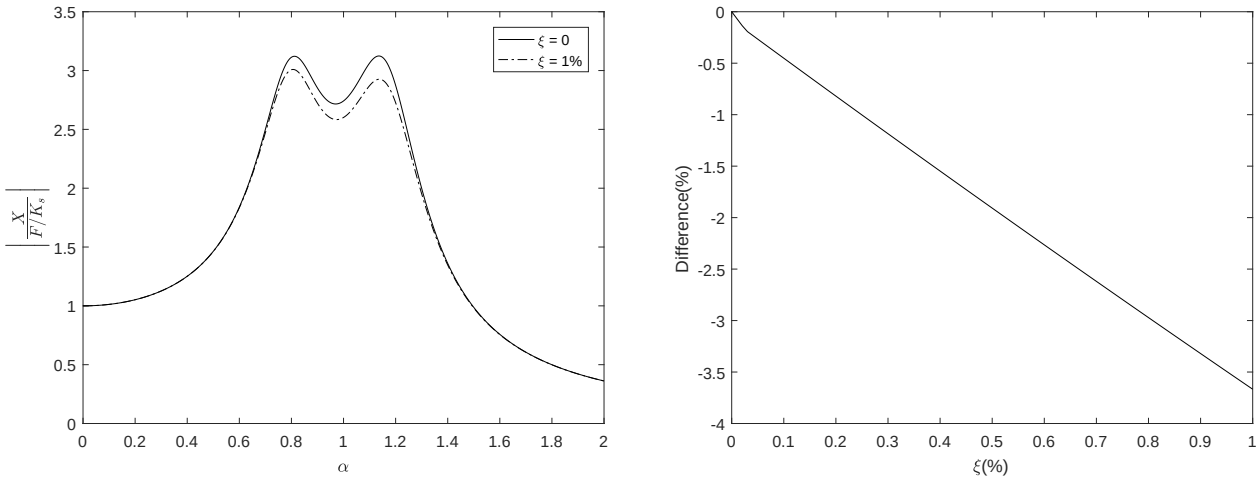


(a) (b)

Figure 10: Influence of mechanical damping ratio $\xi$ of primary system on dynamics response: (a) comparison of frequency responses of primary system without and with viscous damping (solid line: $\xi$ = 0, dash-dotted: $\xi$ = 1%); (b) Difference evolution between peak vibration amplitude of damped and undamped primary system. The shunt circuit parameters are optimized by fixed points theory with inductance ratio $\gamma$ = 0.